$$\frac{\eta(\omega) - \eta_0}{c\eta_0} = \frac{\zeta l^2 N^2 N_A}{\eta_0 M} f_t\left(\frac{cN_A N^{3/2} l^3}{M}, \frac{\omega \zeta l^2 N^2}{k_B T}\right) \quad \text{(III.6)}$$

The scaling predictions for the concentration dependence then follow from (III.4) and (III.5) by using $\nu = {}^1/_2$ as

$$G_N{}^0 \propto (J_e{}^0)^{-1} \propto c^3 \frac{RT}{M_A}\left(\frac{l^3 N_A}{M_A}\right)^2 \quad \text{(III.7)}$$

$$\eta \propto c^{5.8} N^{3.4} \frac{\zeta l^2 N_A}{M_A}\left(\frac{l^3 N_A}{M_A}\right)^{4.8} \quad \text{(III.8)}$$

which yield concentration dependences that are incompatible with experimental data.

IV. Discussion

The scaling approach is used to assess the validity of various physical assumptions concerning the viscoelastic properties of entangled polymer systems. Known molecular weight power law dependences are introduced into the scaling theory to provide predictions for the concentration dependence which, in turn, is compared with experiment. This mode of analysis is applied to three models of the entangled polymer system.

The first model assumes, in effect, that for macroscopically entangled systems there exists a new dimensionless parameter which does not enter into the description of the viscoelastic properties of dilute and semidilute (i.e., nonentanglement limited) solutions. This dimensionless parameter is interpreted, following the review by Graessley,[1] in terms of the chain contact probability. The derived scaling theory concentration dependences of $G_N{}^0$, η, and $J_e{}^0$ are consistent with the experimental data reviewed by Graessley.[1]

The other two models follow the ideas of de Gennes[5] in assuming that the coil overlap concentration, $c_0{}^*$ or c^*, represents the fundamental scaling concentration as it successfully does in the dilute and semidilute regimes.[5,10] Choosing the perturbed (swollen) chain overlap concentration, c^*, provides agreement with recent isothermal data on polybutadiene.[15] However, the high concentrations utilized in the experiment appear to require the use of the unperturbed chain overlap concentration, $c_0{}^*$, as the scaling concentration, and this approach yields scaling predictions which are in poor agreement with experimental values. It should be noted that the c^* scaling model produces an additional predicted solvent quality and temperature dependence of $G_N{}^0$, η, and $J_e{}^0$ through their dependence on the excluded volume, and this is a point which can be tested experimentally. Perhaps there are different possible types of entanglement systems, those where the contact probability provides the scaling concentration, and those for which the coil overlap concentration is the relevant variable. Except for polybutadiene, the available data currently favor the former.

Acknowledgment. I am grateful to Professors Bill Graessley and Masao Doi for helpful discussions and for making their work available to me prior to publication. This research is supported, in part, by National Science Foundation Grant DMR78-26630 (polymers program).

References and Notes

(1) For a review and further references see W. W. Graessley, *Adv. Polym. Sci.*, **16**, 1 (1974).
(2) S. F. Edwards and J. W. Grant, *J. Phys. A: Math., Nucl. Gen.*, **6**, 1169, 1186 (1973).
(3) M. Doi and S. F. Edwards, *J. Chem. Soc., Faraday Trans. 2*, **74**, 1789, 1802 1818 (1978); M. Doi, to be published.
(4) P.-G. de Gennes, "Scaling Concepts in Polymer Physics", Cornell Press, Ithaca, N.Y., 1979, and references therein.
(5) P.-G. de Gennes, *Macromolecules*, **9**, 594 (1976).
(6) S. F. Edwards, *Proc. Phys. Soc., London*, **91**, 513 (1967); *J. Phys. A: Math., Nucl. Gen.*, **1**, 15 (1968).
(7) H. L. Frisch and S. Prager, *J. Chem. Phys.*, **46**, 1475 (1967).
(8) R. T. Deam and S. F. Edwards, *Philos. Trans. R. Soc. London*, **280**, 317 (1976).
(9) K. F. Freed, *J. Chem. Phys.*, **55**, 5588 (1971).
(10) M. K. Kosmas and K. F. Freed, *J. Chem. Phys.*, **69**, 3647 (1978).
(11) R. S. Adler and K. F. Freed, *J. Chem. Phys.*, **70**, 3119 (1979).
(12) R. S. Adler and K. F. Freed, *J. Chem. Phys.*, **72**, 4186 (1980).
(13) K. F. Freed and M. K. Kosmas, *Phys. Rev. B*, **20**, 215 (1979).
(14) F. Bueche, *J. Chem. Phys.*, **25**, 599 (1956).
(15) W. W. Graessley, private communication.
(16) S. F. Edwards, *J. Phys. A: Math., Nucl. Gen.*, **8**, 1670 (1975).

Distribution Functions and Viscoelastic Properties of Perfect Random Nets

J. E. Martin and B. E. Eichinger*

Department of Chemistry, BG-10, University of Washington, Seattle, Washington 98195.
Received January 16, 1980

ABSTRACT: Eigenvalue and relaxation time spectra, viscoelastic properties, mean square dimensions, and the distribution function of the radius of gyration are calculated for perfect networks. These nets consist of a number μ of f-functional junctions connected at random by monodisperse Gaussian chains of $n + 1$ statistical subunits. The dependence of network dimensions on chain length and junction number is determined and it is found that these nets have dimensions which are independent of junction number in the limit of large μ. The viscoelastic functions are calculated from the exact relaxation time spectra near the asymptotic limit $\mu \to \infty$. The results are similar to the Rouse-Mooney static junction theory but cooperative network modes are found which have relaxation times much longer than those of the interlinking chains. The frequency dependences of the storage and loss shear moduli are found to differ in detail from those of the Rouse–Mooney prediction.

Distribution Functions and Mean-Square Dimensions

Previous treatments of the Gaussian network problem have not attempted to account for chain and network cooperative contributions to the mean-square dimensions (MSD) and viscoelastic properties. The reason for this is clear enough; there are many complications in the description of elastic networks. These include the proper

0024-9297/80/2213-0626$01.00/0

choice of the network connectivity, the length distribution of interlinking chains, the effect of dangling chains, loops, and entanglements, and the effect of excluded volume.

Some interesting results have already been obtained for Gaussian networks. Ronca and Allegra[1] studied the MSD of unconstrained crystallographic nets having cyclic boundary condtions and found that in lattices with three-dimensional topology the mean-square distance between any pair of network junctions is virtually independent of their topological separation. As a result the MSD of such nets approach a constant as the number of junctions increases without limit. Following James and Guth[2] they termed this effect network collapse. This result led Ronca and Allegra to conjecture that any network of homogeneous three-dimensional connectivity would experience such a collapse in the ideal Gaussian limit.

Earlier James and Guth[2] treated the crystallographic net in an artificial way that avoided this problem. They applied a set of holonomic constraints to a subset of the network elements, thus fixing the positions of these elements in space. Objections to the unphysical nature of their approach notwithstanding, it is impossible to apply this method to networks of nontrivial connectivity, since the relation between topological position and spatial position is obscure. The theory proposed by Wall[3,4] and elaborated by Flory[5] is based upon assertions which effectively avoid these difficulties. By focusing on the statistics of individual chains and by appealing to the affine deformation of the mean but not the instantaneous junction positions, Flory has produced a comprehensive theory of elasticity which accounts for equilibrium data.

The focus of this contribution is upon the relationship between network connectivity and viscoelastic behavior. Since the long relaxation times that are introduced into polymers upon cross-linking must be the result of network formation, an attempt to understand this aspect of elastomeric behavior necessarily plunges one into the problem of network collapse. An appealing approach to solving the problem of network collapse would be to add a repulsive term to the network potential. Unfortunately, this is difficult for network molecules where high segment densities make the excluded volume effect rather large and difficult to calculate. On the other hand one must ask whether a change of fundamental connectivity, so as to yield nets with a different distribution of small circuits, would prevent the collapse. Since the MSD can be expressed as the first inverse moment of the density of eigenvalues of the Kirchhoff matrix and since this eigenvalue spectrum is highly sensitive to the number of circuits in the network, we can expect to alter the MSD by altering the circuit distribution. In an earlier paper[6] progress was made on this problem by studying a class of regular random networks called reduced nets. A reduced net contains μ junctions of functionality f connected at random by Gaussian bonds. Interlinking chain contributions are not taken into account. In this paper we investigate the perfect random net, which may be obtained from the reduced net by replacing each Gaussian bond by a chain of $n + 1$ segments. Since these nets have random connectivity we are forced to investigate a partial ensemble of the class of perfect nets in order to calculate the properties of interest.

The quantities which we will use to characterize network dimensions are the mean-squared unperturbed radius of gyration, $\langle s^2\rangle_0$, and the distribution function of the reduced radius of gyration $\langle s^2\rangle_0 P(t)$, $t = s^2/\langle s^2\rangle_0$. The radius of gyration is defined as

$$s^2 = N^{-1}\sum_{k=1}^{N}(r_k - N^{-1}\sum_{l=1}^{N} r_l)^2 \qquad (1)$$

where N is the number of elements in the network and r_k is the position vector of the kth element. To obtain a useful expression for $\langle s^2\rangle_0$ we express the bonded potential as

$$V([\mathbf{R}])/kT = \gamma Tr(\mathbf{RKR}^t) \qquad (2)$$

where $\mathbf{R}$ is a $3 \times N$ matrix of the Cartesian coordinates of the N elements, $\mathbf{R}^t$ is its transpose, and $\mathbf{K}$ is the $N \times N$ matrix which describes the connectivity of the network. In eq 2, $\gamma = 3/2\langle l^2\rangle_0$ where $\langle l^2\rangle_0$ is the mean-square bond length. After computing the appropriate configuration integrals, we obtain[7]

$$\langle s^2\rangle_0 = (3/2\gamma N)\sum\lambda^{-1} \qquad (3)$$

$$\langle s^2\rangle_0 P(t) = (2\pi)^{-1}\int_{-\infty}^{+\infty} d\beta \exp(i\beta t)\prod_{k=1}^{N-1}(1 + i\beta/\gamma N\langle s^2\rangle_0\lambda_k)^{-3/2} \qquad (4)$$

where λ_k denotes the kth nonzero eigenvalue of K.

It is difficult to approach the eigenvalue problem for the perfect random net by standard methods. For f-functional nets containing chains of $n + 1$ subunits each the Kirchhoff matrix is of the order $\mu(1 + nf/2)$. In a typical calculation of interest, a tetrafunctional net might consist of 100 junctions connected by chains of 50 elements each. To calculate eigenvalues a 10100×10100 sparse matrix requiring 10^8 storage locations must be diagonalized. On the University of Washington CDC 6400/Cyber 70 computing system the execution time for this calculation would be about 10^3 h. In a previous paper[8] it has been shown how the general network eigenvalue problem can be reduced to manageable proportions. An especially substantial reduction was achieved for perfect nets where the eigenvalue problem is reduced to the diagonalization of a $\mu \times \mu$ Kirchhoff matrix and the subsequent evaluation of the roots of μ trigonometric polynomials. By use of this technique the computing time for the above example is reduced to about 150 s.

The Eigenvalue Problem. The Kirchhoff matrix for a perfect random net may be written in the block form

$$\mathbf{K} = \begin{bmatrix} f\mathbf{1}_\mu & -\mathbf{C} \\ -\mathbf{C}^t & \mathbf{A} \end{bmatrix}$$

where $\mathbf{1}_\mu$ is the identity of rank μ (μ is even) and $\mathbf{A} = \mathbf{1}_{\mu/2} \otimes \mathbf{a}$ where $\mathbf{a} = 2\delta_{i,j} - \delta_{i,j+1} - \delta_{i,j-1}$ is an $n \times n$ matrix which represents the connectivity of a chain. The matrix $\mathbf{C}$, of order $\mu \times \mu nf/2$, specifies the connections between chains and junctions. In partitioned form

$$\mathbf{C} = (\mathbf{C}_1, \mathbf{C}_2, \ldots, \mathbf{C}_{\mu f/2})$$

where $\mathbf{C}_k$ is a $\mu \times n$ matrix. If the kth chain is connected to the ith and jth junctions the elements of $\mathbf{C}_k$ are given by the equation

$$(\mathbf{C}_k)_{l,m} = \delta_{i,l}\delta_{m,1} + \delta_{j,l}\delta_{m,n}$$

Algebraic reduction[5] of the secular equation $|\mathbf{K} - \gamma\mathbf{1}| = 0$ yields the following:

(1) n eigenvalues of degeneracy $\mu(f - 2)/2$ given by

$$\lambda_l = 4\sin^2 \pi l/2(n + 1) \qquad l = 1, 2, \ldots, n \qquad (5)$$

(2) $n\mu$ eigenvalues given by

$$\lambda_{\sigma,l} = 4\sin^2 \theta_{\sigma,l}/2 \qquad (6)$$

where $\theta_{\sigma,l}$ is one of the n real solutions of the trigonometric polynomial of order $n + 1$ given by the equation

$$\cos(n + 3/2)\theta + (f - 1)\cos(n + \tfrac{1}{2})\theta - (f - \kappa_\sigma)\cos\theta/2 = 0 \qquad (7)$$

The κ_σ are μ in number and are just the eigenvalues of the

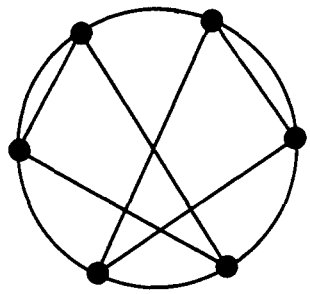

Figure 1. An example of a regular graph which does not conform to eq 8. This is the smallest such tetrafunctional graph, but nonconforming graphs exist for all $\mu \geq 6$.

Kirchhoff matrix of the associated reduced net.

(3) μ eigenvalues obtained from the complex solutions to eq 7, one for each κ_σ. These are very nearly given by $\theta = \pi - i \ln (f - 1)$, and the corresponding eigenvalues are $f^2/(f - 1)$.

The algorithm used to generate the Kirchhoff matrices $\mathbf{K}_r$ for reduced random nets has been given previously,[6] but it is worthwhile to repeat that the $\mathbf{K}_r$ are of the form

$$\mathbf{K}_r = \mathbf{K}_c + \sum_{j=1}^{f-2} \mathbf{P}^t_j (\mathbf{1}_{\mu/2} \otimes \mathbf{B}) \mathbf{P}_j \qquad (8)$$

where $\mathbf{K}_c$ is the Kirchhoff matrix for the circular chain of μ subunits, $\mathbf{P}_j$ is any one of the $\mu!$ permutation matrices, and the matrix $(\mathbf{1}_{\mu/2} \otimes \mathbf{B})$ is the Kirchhoff matrix for μ vertices connected pairwise. The matrix $\mathbf{B}$ is the 2×2 Kirchhoff matrix for two vertices connected by a single edge.

The advantage of generating graphs in this class, rather than trying to generate graphs belonging to the larger class of regular random graphs, is the guarantee that graphs conforming to eq 8 are connected. This results in relatively great computational efficiency since any algorithm generating regular random graphs of N nodes would be required to selectively discard those which are disjoint. Recent theoretical[9] calculations on the density of eigenvalues of regular random graphs indicate that no serious approximation is incurred in limiting consideration to graphs generated by our algorithm. A simple example of a regular random graph not conforming to eq 8 is shown in Figure 1.

Diagonalization of the Kirchhoff matrix $\mathbf{K}_r$ was accomplished by using Householder's[10] method to convert the matrix to a tridiagonal form with subsequent application of the LR algorithm[10] to yield the diagonal matrix. The solutions to eq 7 on the interval $(0,\pi)$ were simply and accurately found by a bisection method. Relative errors in the computed eigenvalues are less than one part in 10^{11}. The eigenvalue spectrum of the perfect random net is determined completely by μ, f, n, and the eigenvalues of the associated reduced random net.

Some calculated spectra of the nondegenerate eigenvalues appear in Figures 2 and 3. A partial list of the numerical results appears in Table I. These are discussed in the following section.

Properties of the Eigenvalue Spectra. To discuss the dependence of the mean-square dimensions on chain length and cross-link number it is useful to obtain a simple expression for the eigenvalue spectra. In the following we let ξ_σ refer to the σth eigenvalue of the adjacency matrix ξ for the reduced random net. For regular f-functional graphs the ξ_σ are related to the eigenvalues of the Kirchhoff matrix by $\xi_\sigma = f - \kappa_\sigma$.

The nondegenerate λ spectra have a simple appearance. Each spectrum consists of n bands of μ eigenvalues each,

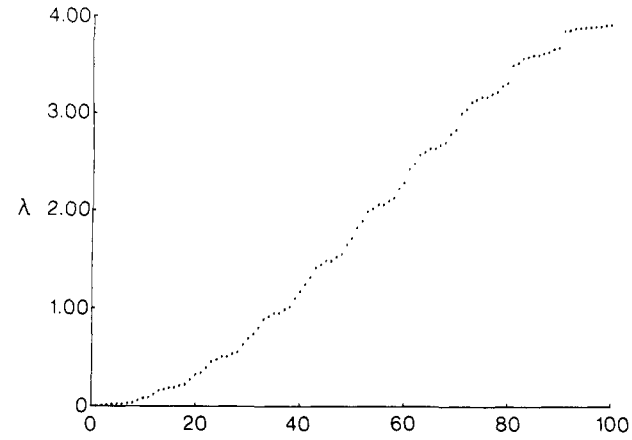

Figure 2. A nondegenerate eigenvalue spectrum for a trifunctional net having $\mu = 10$, $n = 10$. In this low μ limit the eigenvalues are not clearly separated into bands.

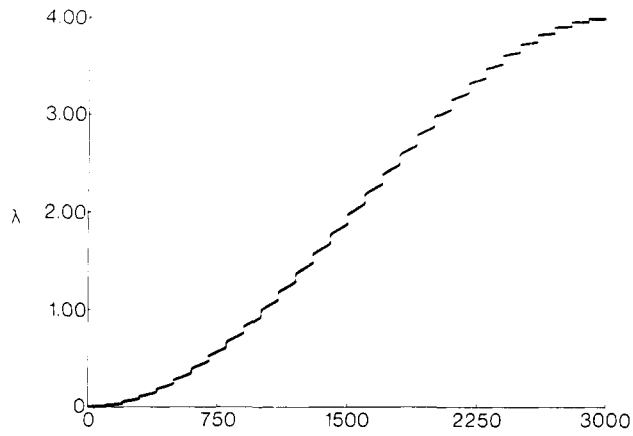

Figure 3. A nondegenerate eigenvalue spectrum for a trifunctional net having $\mu = 100$, $n = 30$. The plot contains 3000 eigenvalues, the 30 bands having 100 eigenvalues each.

Table I

f	μ	n	N	A^a	B^b	C^c
4	100	10	2100	4.93	0.155	1.349
4	100	20	4100	9.39	0.562	1.342
4	100	30	6100	13.85	1.22	1.340
4	100	50	10100	22.90	3.38	1.347
3	100	10	1600	7.64	0.724	2.089
3	100	20	3100	14.58	2.64	2.084
3	100	30	4600	21.51	5.74	2.082
3	100	50	7600	35.38	15.54	2.082
4	10	10	210	4.09	0.910	
4	20	10	420	4.41	0.504	
4	60	10	1260	4.73	0.222	
4	100	10	2100	4.93	0.155	
3	10	10	160	5.56	3.35	
3	20	10	320	7.06	3.12	
3	40	10	640	7.10	1.44	
3	100	10	1600	7.64	0.724	

[a] $A = \langle s^2 \rangle_0 / \langle l^2 \rangle_0$. [b] $B = (\langle s^4 \rangle_0 - \langle s^2 \rangle_0^2) / \langle l^2 \rangle_0^2$. [c] $C = \langle s^2 \rangle_0 / \langle l^2 \rangle_0 n'(1 - 1/n'^2)/6$.

the σth eigenvalue in the lth band arising from the lth solution to eq 7 with ξ_σ fixed. We use the convention that the ξ_σ are a monotonic nonincreasing function of σ. This suggests that the lth band of eigenvalues is of the form

$$\lambda_{\sigma,l} = a_l + b_l \xi_\sigma \qquad (9)$$

where $\lambda_{\sigma,l}$ is the $(\mu(l - 1) + \sigma)$th eigenvalue in the nondegenerate λ spectrum. Since the ξ_σ lie nearly symmetrically about zero on the interval $(-2(f - 1)^{1/2}, 2(f - 1)^{1/2})$ we are

led to seek the n solutions θ_l to eq 7 with $\xi_\sigma = 0$ and to expand the solutions $\theta_{l,\sigma}$ in terms of the ξ_σ near these θ_l. This leads to

$$\lambda_{\sigma,l} = 4 \sin^2 (\theta_{\sigma,l}/2); \theta_{\sigma,l} \simeq \theta_l + \left.\frac{d\theta}{d\xi_\sigma}\right|_{\theta=\theta_l} \xi_\sigma \quad (10)$$

$$\lambda_{\sigma,l} = 4 \sin^2 (\theta_l/2) - 2 \sin \theta_l \left.\frac{d\theta}{d\xi_\sigma}\right|_{\theta=\theta_l} \xi_\sigma \quad (11a)$$

$$\frac{d\theta}{d\xi_\sigma} = \cos (\theta/2)/[{}^1/_2 \tan (\theta/2) \times (\cos (n + {}^3/_2)\theta + (f - 1) \cos (n + {}^1/_2)\theta) - (n + {}^3/_2) \sin (n + {}^3/_2)\theta - (f - 1)(n + {}^1/_2) \sin (n + {}^1/_2)\theta] \quad (11b)$$

In finding the θ_l we seek high accuracy for small θ_l as the smallest eigenvalues make the largest contributions to $\langle s^2 \rangle_0$. We assume a solution of the form $\theta_l = \pi l/(2n + \alpha)$, $l = 1, 3, 5, \ldots, 2n - 1$, and substitute this into eq 7 to obtain

$$\sin \frac{(3 - \alpha)\pi l}{2(2n + \alpha)} + (f - 1) \sin \frac{(1 - \alpha)\pi l}{2(2n + \alpha)} = 0 \quad (12)$$

$$\theta_l = \pi l/(2n + 2/f + 1)$$

For $n = 10$, this gives values of θ_l which are accurate to one part in 10^5 for small l and for large l are no worse than one part in 10^2. For large n the agreement becomes even better.

This accurate representation of the λ spectrum can be used to calculate eigenvalue density distributions and other properties of interest. The dependence of $\langle s^2 \rangle_0$ on the chain length can be obtained by further approximation. Equation 9 can be used in eq 3 to yield the expansion

$$\sum_{\sigma=1}^{\mu} 1/\lambda_{\sigma,l} = a_l^{-1} \sum_{p=0}^{\infty} (-1)^p (b_l/a_l)^p P_{Tr}(\xi^p) = (1/\lambda_l)(\mu + 0 + \mu f(b_l/a_l)^2 + 6T(b_l/a_l)^3 + \ldots) \simeq \mu/\lambda_l; \quad \lambda_l \equiv 4 \sin^2 \theta_l/2 \quad (13)$$

where T is the number of triangles in the reduced graph[11] and is independent of μ.[9] For tetrafunctional nets it suffices to approximate $\theta_l = \pi l/(n + {}^3/_2) \simeq \pi l/(2n + 2)$. Combining this with the contribution from the degenerate eigenvalues, having set $f^2/(f - 1)$ to 4 $\sin^2 (\pi/2)([2n + 1]/[2n + 2])$, we arrive at an approximate μ-fold degenerate eigenvalue spectrum from which the dependence of $\langle s^2 \rangle_0$ on n can be found. The moment generating function for the radius of gyration becomes[12] the following with these approximate eigenvalues:

$$M(\beta) = \langle e^{i\beta s^2} \rangle = (\prod_{l=1}^{n'-1} \lambda_l)^{3\mu/2} U_{n'-1}{}^{-3\mu/2}(1 + i\beta/2\gamma' n') \quad (14)$$

where $n' = 2n + 2$, $\gamma' = \gamma\mu(2n + 1)/(2n + 2)$, and $U_{n'-1}$ is the Chebyshev polynomial of order $n' - 1$. Thus we obtain

$$\langle s^2 \rangle_0 / \langle l^2 \rangle_0 = \frac{n'}{6}(1 - 1/n'^2) \quad (15)$$

Table I compares the values of $\langle s^2 \rangle_0/\langle l^2 \rangle_0$ computed from eq 3 with this expression. The two agree to within a multiplicative constant even for trifunctional perfect nets.

In considering the μ dependence of the mean-square dimensions it is helpful to consider each set of eigenvalues, degenerate and nondegenerate, separately. The contribution of the degenerate eigenvalues to $\langle s^2 \rangle_0/\langle l^2 \rangle_0$ is given by

$$((f - 2)/(nf + 2)) \sum_{l=1}^{n} 1/(4 \sin^2 (\pi l/2n + 1)) + (f - 1)/f^2(1 + nf/2) \quad (16)$$

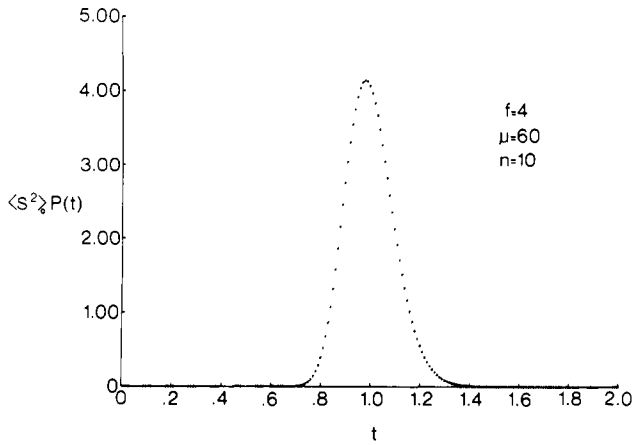

Figure 4. $\langle s^2 \rangle_0 P(t)$ plotted on the relative t axis. Fluctuations of s^2 from its mean value are small. The numerical calculation was performed without approximation of the eigenvalue spectrum.

which contains no dependence on μ. Any μ dependence must arise from the nondegenerate λ spectrum. We shall now find a set of eigenvalues $\xi_{l,\sigma}$ such that $\epsilon_{l,\sigma} \leq \lambda_{l,\sigma}$; these can then be used to set an upper bound to the contribution of the nondegenerate eigenvalues to $\langle s^2 \rangle_0$. These are obtained by linearizing eq 7 to obtain a good estimate for the $\lambda_{1,\sigma}$ band of eigenvalues. The result is

$$\epsilon_{1,\sigma} = 2(f - \xi_\sigma)/(n^2 f + (f + 2)n + 2 + f/2) \leq \lambda_{1,\sigma} \quad (17)$$

The inequality can be shown to hold by substituting eq 17 into eq 7 and noting that the sign of eq 7 does not change on $[0,\theta_{1,\sigma}]$ where $\theta_{1,\sigma} \simeq \epsilon_{1,\sigma}{}^{1/2}$. Now since $\lambda_{l,\sigma} > \lambda_{1,\sigma} \geq \epsilon_{1,\sigma}$ for $2 \leq l \leq n$, we let $\epsilon_{l,\sigma} = \epsilon_{1,\sigma}$ for all l to obtain a set of eigenvalues consistent with obtaining an upper bound for the MSD. This yields

$$\lim_{\mu \to \infty} \langle s^2 \rangle_0 / \langle l^2 \rangle_0 < \lim_{\mu \to \infty} (\text{constant}/\mu) \sum_{\sigma=1}^{\mu=1} (f - \xi_\sigma)^{-1} = C_{f,n} \quad (18)$$

The evaluation of the sum in eq 18 has been accomplished in a previous paper[6] on reduced nets and it is there shown that $C_{f,n}$ does not depend on μ if $f > 2$. This result shows that perfect nets collapse and that the dimensions of nets with monodisperse chains are so intimately related to the dimensions of the associated reduced net that the latter must be studied prior to the more complete investigation of networks with chain modes included. This line of attack will be pursued in future work.

In Figure 4 a sample distribution function of the reduced radius of gyration is shown for a tetrafunctional net. This distribution function is much narrower than that of the linear or circular chain, showing that relative fluctuations of s^2 tend to be small for perfect nets. Surprisingly, this distribution function is narrower than that of the reduced random graph of the same junction number.

From these results it is clear that the network collapse must have as its underlying cause either the omission of spatial constraints in the network connectivity or the lack of repulsive terms in the network potential. Current calculations[13] and theoretical work[14] on networks with spatial constraints acting at the time of formation strongly suggest that the excluded volume effect is crucial to the support of networks against contractive collapse.

Dynamic Properties

Theoretical work on the viscoelastic properties of Gaussian networks has heretofore been based on Rouse–Mooney theory. Following Kirkwood's[15] treatment of the configurational diffusion of a polymer molecule, Rouse[16]

formulated a theory for the dynamic viscosity of a linear Gaussian chain in a sinusoidal shear field. From this Rouse obtained the Gaussian contribution to the spectrum of relaxation times $H(\tau)$ and found that $H(\tau) \propto \tau^{-1/2}$ and that both the storage and loss parts of the complex shear modulus, $G(\omega)$, were proportional to $\omega^{1/2}$ in the frequency range where Gaussian modes can be expected to account for $G(\omega)$. Zimm[17] extended the Rouse treatment by including the preaveraged Oseen hydrodynamic interactions and found that $H(\tau) \propto \tau^{-2/3}$. Bueche[18] suggested that the molecular theory intially formulated for dilute polymer solutions could be extended to the bulk, undiluted state if the subunit friction factor is appropriately modified and if the theory is confined to chains of sufficiently low molecular weight so that entanglement coupling can be ignored. Finally, Mooney[19] formulated a static cross-link model of a polymer network, in which the only relaxation processes stem from the configurational diffusion of a linear Gaussian chain constrained at both ends. The relaxation times that Mooney found are just the Rouse relaxation times, to which he added one infinite relaxation time to account for the nonzero equilibrium modulus.

We believe that the first step in extending the Rouse theory to networks should be taken without making any special assumptions regarding separation of chain and junction modes, or regarding differences between friction factors of junctions and chain segments. We thus find a complicated spectrum of relaxation times, which includes contributions from chain motions, cooperative network motions, and even motions of the network junctions themselves.[20] Relaxation times much longer than those of the Rouse–Mooney theory are found and these will be shown to yield a somewhat different dependence of the complex shear modulus on ω.

Viscoelastic Properties. The generalization of the Rouse–Zimm treatment of a linear polymer in a shear field to polymers of arbitrary complexity requires only the computation of the spectrum of relaxation times; the fundamental theory remains intact. Since these relaxation times are independent of the driving force on the system they may be obtained from the equations of motion. The x component of the equation of motion of a Gaussian molecule in a viscous medium is

$$m\ddot{\mathbf{x}} = -\zeta\,\dot{\mathbf{x}} - 2\gamma kT\mathbf{K}\mathbf{x} + \mathbf{A}(t) \qquad \mathbf{x} = (x_1, x_2, \ldots, x_N) \tag{19}$$

where ζ is the subunit friction factor and $\mathbf{A}(t)$ is the Brownian force. A normal coordinate transformation decouples eq 19 to yield

$$m\ddot{q}_j = -\zeta q_j - 2\gamma kT\lambda_j q_j + a(t) \tag{20a}$$

For motions having long relaxation times the inertial term may be neglected, giving the Langevin equation

$$\zeta\dot{q}_j = -2\gamma kT\lambda_j q_j + a(t) \tag{20b}$$

The solution to this stochastic differential equation is $\rho_j(q_j,t)$, the configurational distribution function of the jth normal coordinate. This arises as the solution to the associated Fokker–Planck equation[21]

$$\frac{\partial}{\partial t}\rho_j(q_j,t) = (1/\tau_j')\langle q_j^2\rangle\frac{\partial^2}{\partial q_j^2}\rho_j(q_j,t) + \frac{\partial}{\partial q_j}q_j\rho_j(q_j,t) \tag{21a}$$

It can be shown that if the distribution $\rho_j(q_j,t)$ is perturbed from its equilibrium value it relaxes exponentially with a characteristic decay time

$$\tau_j' = \zeta/2kT\gamma\lambda_j \tag{21b}$$

Mooney[19] has explicity shown this for the instantaneous triaxial strain $\alpha_{ij} = \alpha_i\delta_{ij}$. In general, the relaxation times appropriate to the calculation of a particular molecular property can be related to those of eq 21b.[17] The relaxation times which are useful for the calculation of viscoelastic properties are given by $\tau_j = \tau_j'/2$. To calculate the shear viscoelastic properties of the perfect net we simply apply this spectrum of relaxation times, calculated from the eigenvalue spectrum, to the standard results of molecular and phenomenological[22] viscoelastic theory.

When a shear strain $\gamma(t)$ is applied to a viscoelastic system, the shear stress is determined by

$$\sigma(t) = \int_{-\infty}^{t} G(t - t')\dot{\gamma}(t')\,dt' \tag{22}$$

In terms of the logarithmic density of relaxation times, $H(\tau)$, the relaxation modulus $G(t)$ may be written as

$$G(t) = G_e + G_s\int_{-\infty}^{+\infty} H(\tau)e^{-t/\tau}\,d\ln\tau \tag{23}$$

where G_s is the equilibrium part of $G(t)$. The logarithmic density of eigenvalues is

$$H(\tau) = \sum_{i=1}^{N-1}\tau\delta(\tau - \tau_i) \tag{24a}$$

$$\int H(\tau)\,d\ln\tau = N - 1 \tag{24b}$$

The relaxation modulus may be written in terms of $g(\lambda)$, the density of eigenvalues, with the dynamic part appearing as

$$G(t) = G(t) - G_e = (N-1)G_s\int_0^\infty g(\lambda)e^{-\lambda/\alpha}\,d\lambda \tag{25a}$$

$$\int_0^\infty g(\lambda)\,d\lambda = 1; \qquad \alpha = \zeta/4kT\gamma \tag{25b}$$

Finally the complex shear modulus may be written

$$G(\omega) = G_s\int_{-\infty}^{+\infty}\frac{\omega\tau}{1 + i\omega\tau}H(\tau)\,d\ln\tau \tag{26}$$

In evaluating these quantities for networks, we are careful to note that although $G(\omega)$ and $G(t)$ are intensive properties, the normalization in eq 24 seems to indicate an apparent μ dependence in the viscoelastic properties. This can be removed by considering G_s as a μ dependent variable and by taking the limit as $\mu \to \infty$. In this way

$$G_sH(\tau) = \tilde{g}\tilde{H}(\tau) \tag{27a}$$

$$\tilde{H}(\tau) = \lim_{\mu\to\infty}(1/\mu)\sum_{i=1}^{N-1}\tau\delta(\tau - \tau_i) \tag{27b}$$

$$\int_{-\infty}^{+\infty}\tilde{H}(\tau)\,d\ln\tau = nf/2 + 1 \tag{27c}$$

where $\tilde{g}$ is a constant which depends only upon the intensive properties of the substance. While the logarithmic density of nondegenerate eigenvalues may be considered to be a function in this limit (see Figure 5), the logarithmic density of degenerate eigenvalues may not. This latter contribution is

$$\lim_{\mu\to\infty}(1/\mu)\sum_{l=1}^{n+1}\mu\frac{(f-2)}{2}\tau\delta(\tau - \tau_l) = \sum_{l=1}^{n+1}\frac{(f-2)}{2}\tau\delta(\tau - \tau_l) \tag{28}$$

where $\mu(f-2)/2$ is the degeneracy of the lth eigenvalue. This unfortunate result is due to the uniform chain length in the perfect net.

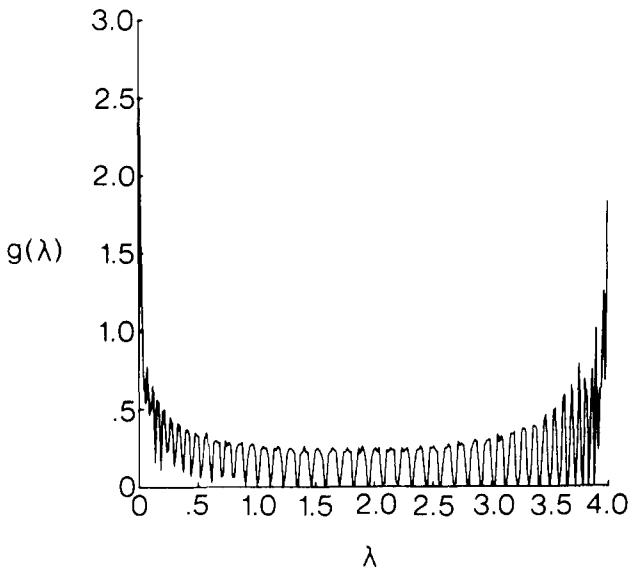

Figure 5. The nondegenerate density of eigenvalues for a large trifunctional net having $\mu = 100$, $n = 50$. The function $g(\lambda)$ was calculated directly from the net eigenvalue spectrum by counting the number of eigenvalues on the interval $[\lambda,\lambda + d\lambda]$. Normalization is according to eq 25b.

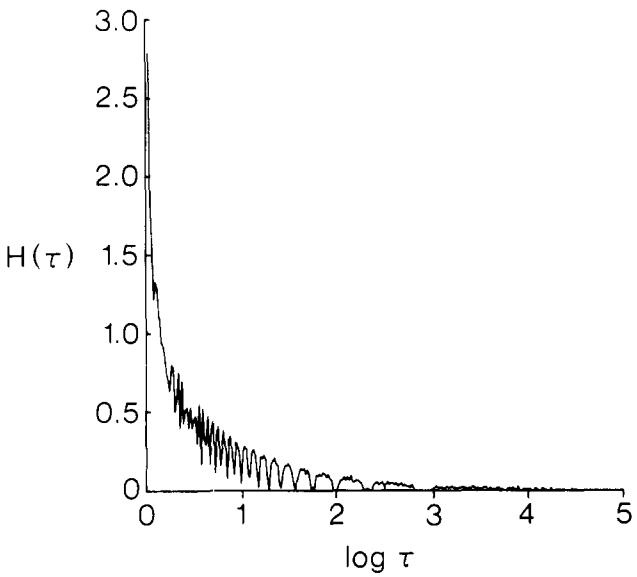

Figure 6. The logarithmic density of nondegenerate relaxation times calculated for the net used in Figure 5. $H(\tau)$ was calculated directly from the relaxation time spectrum by counting the number of relaxation times on the interval $[\ln \tau, \ln \tau + d \ln \tau]$. For convenience we have set $\tau_j = 4/\lambda_j$ and have normalized the integral of $H(\tau)$ to unity.

A pictorial representation of $H(\tau)$ which is also useful for calculating the above viscoelastic properties may be obtained by a smoothing technique. A change of variables to $\nu = 1/\tau$ casts eq 23 into the form of a Laplace transformation. Application of the Widder–Post inversion formula yields[23]

$$H(\tau) = \lim_{k\to\infty} \frac{(-t)^k}{(k-1)!} \frac{d^k G(t)}{dt^k}\bigg|_{t=k\tau} = \lim_{k\to\infty} \frac{k^k}{(k-1)} \sum_{i=1}^{N-1} (\tau/\tau_i) \exp(-k\tau/\tau_i) \qquad (29)$$

which gives an approximate smoothed $H_k(\tau)$ for finite k. The function $H_k(\tau)$ was calculated for values of k in the range 2–1000 but $k = 8$ gave reasonably smooth density functions which could be used to calculate viscoelastic

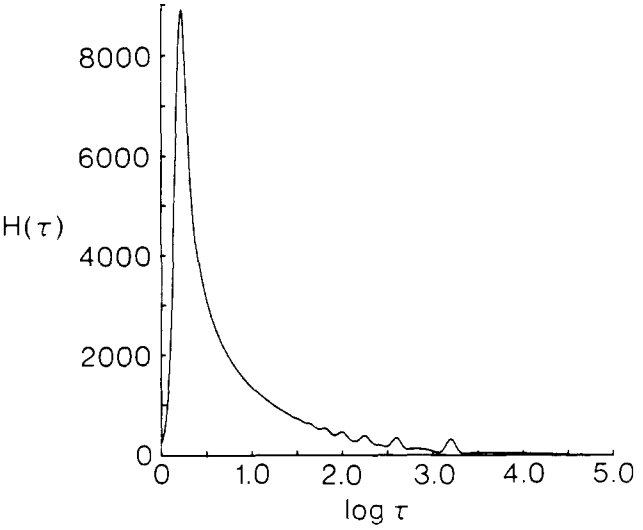

Figure 7. The smoothed logarithmic density of relaxation times, both degenerate and nondegenerate, calculated for a tetrafunctional net having $\mu = 100$, $n = 50$. This $H_k(\tau)$ was calculated from eq 29 with $k = 64$. In this plot the relaxation times were calculated as $\tau_i = 6/\lambda_i$.

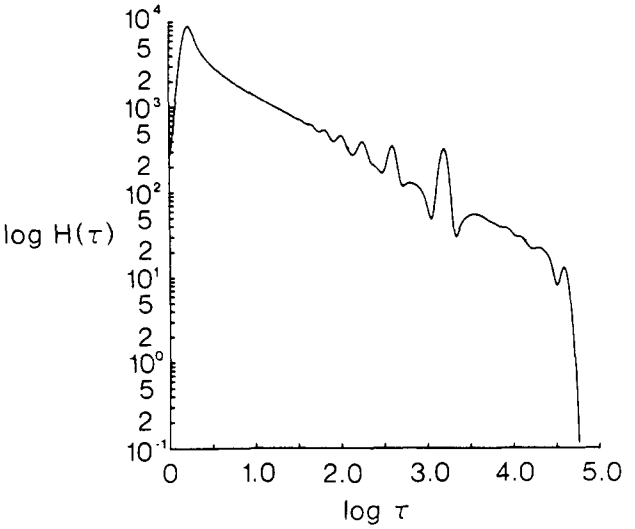

Figure 8. A logarithmic plot of the $H_k(\tau)$ in Figure 7.

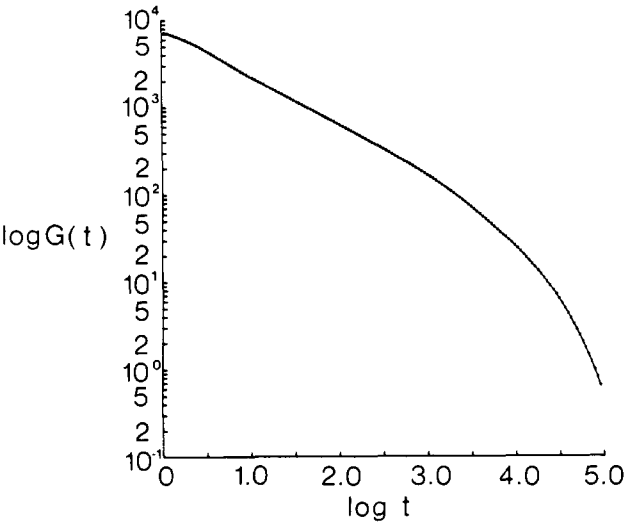

Figure 9. The logarithm of the dynamic part of the shear relaxation modulus calculated from eq 23. The solid line represents the exact $G(t)$ calculated from the $H(\tau)$ given in eq 24a whereas the points are derived from the approximate $H_k(\tau)$ in Figure 7. The two methods of computation agree well with one another.

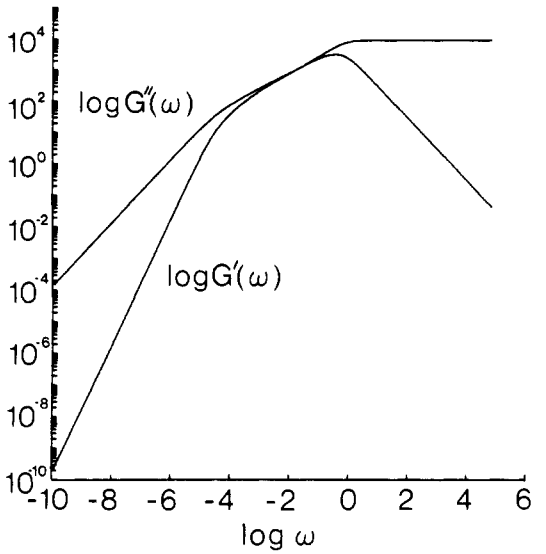

Figure 10. The frequency dependent parts of the storage and loss components of the complex shear modulus are plotted logarithmically. The frequency axis is arbitrary since we have arbitrarily chosen the constant of proportionality between τ_j and $1/\lambda_j$. The Gaussian model is inadequate at high frequencies and this portion of the graph can be ignored.

properties with high accuracy. Graphs of $H_k(\tau)$ and $G_k(t)$ calculated in this manner for tetrafunctional nets are shown in Figures 7–9. We have calculated $G(t)$ and $G(\omega)$ directly from the relaxation spectra; these appear in Figures 9 and 10. We also find that the ratio of the longest cooperative network relaxation time to the longest Rouse–Mooney relaxation time for an interlinking chain is

$$\rho \equiv \tau_{max}^{net}/\tau_{max}^{chain} \simeq \pi^2(f + (f+2)/n)/2(f - 2(f-1)^{1/2}) \quad (30)$$

where eq 18 has been used with min $(f - \xi_\sigma) = f - 2(f - 1)^{1/2}$.[12] For tetrafunctional nets this yields $\rho \simeq 37(1 + 3/2n)$ whereas for trifunctional nets $\rho = 87(1 + 5/3n)$.

The approximate slope of the smoothed $H(\tau)$ shown in Figure 8 indicates that within the range $\tau_{min} \leq \tau \leq \tau_{max}$, $H(\tau) \propto \tau^{-0.54}$ for tetrafunctional nets and for trifunctional nets $H(\tau) \propto \tau^{-0.53}$, although these are gross approximations to the true spectra. Finally, for both trifunctional and tetrafunctional nets $G'(\omega) \propto \omega^{0.57}$ and $G''(\omega) \propto \omega^{0.50}$ in the region $1/\tau_{max} \leq \omega < 1/\tau_{min}$. This differs from Rouse–Mooney theory, for which $G'(\omega) \propto G''(\omega) \propto \omega^{1/2}$ in a region which does not extend as far into the low-frequency regime as do the results reported here. A result of these calculations which differs markedly from previous work is that the relaxation times associated with network junctions are given by $\alpha(f-1)/f^2$, which are the shortest relaxation times in the net. There are μ such times, one for each junction. By comparison of the results on the eigenvalues and eigenvectors of stars these can be associated with fast junction motions. This contrasts strongly with Rouse–Mooney theory where the junctions are treated as static points.

References and Notes

(1) G. Ronca and G. Allegra, *J. Chem. Phys.*, **63**, 4104 (1975).
(2) H. M. James and E. Guth, *J. Chem. Phys.*, **15**, 669 (1947).
(3) F. T. Wall, *J. Chem. Phys.*, **10**, 485 (1942).
(4) F. T. Wall, *J. Chem. Phys.*, **11**, 527 (1943).
(5) P. J. Flory and J. Rehner, *J. Chem. Phys.*, **11**, 512 (1943).
(6) J. E. Martin and B. E. Eichinger, *J. Chem. Phys.*, **69**, 4588 (1978).
(7) B. E. Eichinger, *Macromolecules*, **5**, 496 (1972).
(8) B. E. Eichinger and J. E. Martin, *J. Chem. Phys.*, **69**, 4595 (1978).
(9) B. D. McKay, Mathematics Research Report No. 9, University of Melbourne, 1979.
(10) E. Isaacson and H. B. Keller, "Analysis of Numerical Methods", Wiley, New York, 1966.
(11) M. Behzad and G. Chartrand, "Introduction to the Theory of Graphs", Allyn and Bacon, Boston, 1972.
(12) S. R. Coriell and J. L. Jackson, *J. Math. Phys.*, **8**, 1276 (1967).
(13) B. E. Eichinger, University of Washington, work in progress.
(14) B. D. McKay, University of Melbourne, private communication.
(15) J. G. Kirkwood, *Recl. Trav. Chim. Pays-Bas*, **68**, 649 (1949).
(16) P. E. Rouse, *J. Chem. Phys.*, **21**, 1272 (1953).
(17) B. H. Zimm, *J. Chem. Phys.*, **24**, 269 (1956).
(18) F. Bueche, *J. Chem. Phys.*, **20**, 1959 (1952).
(19) M. Mooney, *J. Polym. Sci.*, **34**, 599 (1959).
(20) B. E. Eichinger and J. E. Martin, *J. Polym. Sci., Polym. Lett. Ed.*, **17**, 209 (1979).
(21) M. C. Wang and G. E. Uhlenbeck, *Rev. Mod. Phys.*, **17**, 323 (1945).
(22) J. D. Ferry, "Viscoelastic Properties of Polymers", 2nd ed., Wiley, N.Y., 1970.
(23) N. W. Tschoegl, *Rheol. Acta*, **10**, 595 (1971).